ISSN 1674-1056
http://cpb.iphy.ac.cn
http://iopscience.iop.org/cpb
中国物理 B
Chinese Physics
中国物理 Chinese Physics B

Transport properties of topological nodal-line semimetal candidate $CaAs_3$ under hydrostatic pressure

Jing Li(李婧), Ling-Xiao Zhao(赵凌霄), Yi-Yan Wang(王义炎), Xin-Min Wang(王欣敏), Chao-Yang Ma(麻朝阳), Wen-Liang Zhu(朱文亮), Mo-Ran Gao(高默然), Shuai Zhang(张帅), Zhi-An Ren(任治安), Gen-Fu Chen(陈根富)

Citation: Chin. Phys. B . 2019, 28(4): 046202. **doi:** 10.1088/1674-1056/28/4/046202
Journal homepage: http://cpb.iphy.ac.cn; http://iopscience.iop.org/cpb

What follows is a list of articles you may be interested in

Phase transitions in bismuth under rapid compression

Dong-Liang Yang(杨栋亮), Jing Liu(刘景), Chuan-Long Lin(林传龙), Qiu-Min Jing(敬秋民), Yi Zhang(张毅), Yu Gong(宫宇), Yan-Chun Li(李延春), Xiao-Dong Li(李晓东)

Chin. Phys. B . 2019, 28(3): 036201. **doi:** 10.1088/1674-1056/28/3/036201

Shock temperature and reflectivity of precompressed H_2O up to 350 GPa:Approaching the interior of planets

Zhi-Yu He(贺芝宇), Hua Shu(舒桦), Xiu-Guang Huang(黄秀光), Qi-Li Zhang(张其黎), Guo Jia(贾果), Fan Zhang(张帆), Yu-Chun Tu(涂昱淳), Jun-Yue Wang(王寓越), Jun-Jian Ye(叶君建), Zhi-Yong Xie(谢志勇), Zhi-Heng Fang(方智恒), Wen-Bing Pei(裴文兵), Si-Zu Fu(傅思祖)

Chin. Phys. B . 2018, 27(12): 126202. **doi:** 10.1088/1674-1056/27/12/126202

Unusual softening behavior of yield strength in niobium at high pressures

Qiu-Min Jing(敬秋民), Qiang He(何强), Yi Zhang(张毅), Shou-Rui Li(李守瑞), Lei Liu(柳雷), Qi-Yue Hou(侯琪玥), Hua-Yun Geng(耿华运), Yan Bi(毕延), Yu-Ying Yu(俞宇颖), Qiang Wu(吴强)

Chin. Phys. B . 2018, 27(10): 106201. **doi:** 10.1088/1674-1056/27/10/106201

Pressure-induced enhancement of optoelectronic properties in PtS_2

Yi-Fang Yuan(袁亦方), Zhi-Tao Zhang(张志涛), Wei-Ke Wang(王伟科), Yong-Hui Zhou(周永惠), Xu-Liang Chen(陈绪亮), Chao An(安超), Ran-Ran Zhang(张冉冉), Ying Zhou(周颖), Chuan-Chuan Gu(顾川川), Liang Li(李亮), Xin-Jian Li(李新建), Zhao-Rong Yang(杨昭荣)

Chin. Phys. B . 2018, 27(6): 066201. **doi:** 10.1088/1674-1056/27/6/066201

Exploring the compression behavior of HP-$BiNbO_4$ under high pressure

Yin-Juan Liu(刘银娟), Jia-Wei Zhang(张佳威), Duan-Wei He(贺端威), Chao Xu(许超), Qi-Wei Hu(胡启威), Lei Qi(戚磊), A-Kun Liang(梁阿坤)

Chin. Phys. B . 2017, 26(11): 116202. **doi:** 10.1088/1674-1056/26/11/116202

SPECIAL TOPIC — Topological semimetals

Transport properties of topological nodal-line semimetal candidate $CaAs_3$ under hydrostatic pressure*

Jing Li(李婧)[1,2], Ling-Xiao Zhao(赵凌霄)[1], Yi-Yan Wang(王义炎)[1], Xin-Min Wang(王欣敏)[1,2], Chao-Yang Ma(麻朝阳)[1], Wen-Liang Zhu(朱文亮)[1,2], Mo-Ran Gao(高默然)[1,2], Shuai Zhang(张帅)[1], Zhi-An Ren(任治安)[1,2,3] and Gen-Fu Chen(陈根富)[1,2,3,†]

[1] *Institute of Physics and Beijing National Laboratory for Condensed Matter Physics, Chinese Academy of Sciences, Beijing* 100190, *China*
[2] *School of Physical Sciences, University of Chinese Academy of Sciences, Beijing* 100049, *China*
[3] *SongShan Lake Materials Laboratory, Dongguan* 523808, *China*

(Received 25 January 2019; revised manuscript received 25 February 2019; published online 19 March 2019)

We report the transport properties of the $CaAs_3$ single crystal, which has been predicted to be a candidate for topological nodal-line semimetals. At ambient pressure, $CaAs_3$ exhibits semiconducting behavior with a small gap, while in some crystals containing tiny defects or impurities, a large "hump" in the resistivity is observed around 230 K. By applying hydrostatic pressure, the samples appear to a tendency towards metallic behavior, but not fully metallized up to 2 GPa. Further high pressure studies are needed to explore the topological characteristics for $CaAs_3$.

Keywords: hydrostatic pressure, topological material, crystal growth

PACS: 62,.50.–p, 72.20.–i, 05.30.Rt **DOI:** 10.1088/1674-1056/28/4/046202

1. Introduction

The discovery of topological semimetals (TSMs) has attracted broad attention in condensed matter physics and material science because of the topologically protected band structure. TSMs give rise to some exotic physical properties, including giant magnetoresistance (MR), ultrahigh carrier mobility, nontrivial Berry phase, and negative longitudinal MR.[1–4] According to the degeneracy of the band crossing points and their distribution in the Brillouin zone (BZ), TSMs can classify into Dirac semimetals (DSMs), Weyl semimetals (WSMs), and nodal-line semimetals (NLSMs).[5] The band crossing points are four-fold degenerate for DSMs, such as Na_3Bi and Cd_3As_2.[6–8] WSMs exhibit two-fold degenerate band crossing points with definite chirality, and it is located at an even number of discrete points in the BZ, such as TaAs[9,10] and WTe_2.[11,12] Different from the discrete points in DSMs and WSMs, the band crossing points form closed loops in the BZ of NLSMs.[13,14]

Recently, it has been reported that black phosphorus (BP) exhibits a topological phase transition from band semiconductor to zero-gap Dirac semimetal state[15,16] under hydrostatic pressure. The semimetal phase in BP is characterized by the large MR, the coexistence of electron and hole pockets, low carrier densities, small cyclotron masses, weak localization-weak antilocalization transition at low magnetic fields and the emergence of a nontrivial Berry phase of π detected by Shubnikov-de Haas (SdH) magneto-oscillations. BP has a puckered honeycomb lattice,[17–19] in which the direct band gap is mainly determined by the out-of-plane p_z-like orbital of P and can be further reduced by tuning the interlayer coupling.[15,20,21] Interestingly, in $CaAs_3$, the two-dimensional infinite polyanionic As_3^{2-} nets are derivatives of the BP structure. While a deeper and systematic study on $CaAs_3$ single crystals is still missing except for the semiconducting behavior.[22,23] More recently, $CaAs_3$ was predicted theoretically to be a candidate for topological insulator (TI) or NLSMs when the spin–orbit coupling (SOC) was taken into consideration or not and the topological transition could be engineered via strain, or chemical doping.[5,24] While it should be degenerate to a strong topological insulator (TI) with taking the SOC into consideration.[5,24] Hydrostatic pressure has been recognized as a powerful tool for studying band structures of semiconductors. Therefore, combined with the theoretical prediction, it is necessary to study the pressure effect on the transport properties of $CaAs_3$.

In this work, we have grown the single crystals of $CaAs_3$ and performed the studies of transport properties at atmospheric and hydrostatic pressures. $CaAs_3$ shows a semiconducting-like behavior at atmospheric pressure. A large hump in the resistivity is also observed for some crystals containing tiny defects or impurities. Hydrostatic pressure can effectively reduce its resistivity, but it is not fully metallized

*Project supported by the National Key Research and Development Program of China (Grant Nos. 2016YFA0401000 and 2016YFA0300604), the National Key Basic Research Program of China (Grant No. 2015CB921303), the Strategic Priority Research Program (B) of Chinese Academy of Sciences (Grant No. XDB07020100), and the National Natural Science Foundation of China (Grant No. 11874417).

†Corresponding author. E-mail: gfchen@iphy.ac.cn

© 2019 Chinese Physical Society and IOP Publishing Ltd

up to 2 GPa. However, a small drop of resistivity is observed above 1.5 GPa for some samples, indicating the onset of superconducting transition.

2. Experiment and method

Single crystals of $CaAs_3$ were grown by the modified Bridgman method. Firstly, stoichiometric amounts of Ca and As granule were put into an Al_2O_3 crucible, and sealed in an evacuated quartz ampule, which was then heated extremely slowly and kept at 900 °C for 10 h before turning the furnace off. Secondly, the precursor was grinded, tableted, put into an Al_2O_3 crucible, and then sealed again as described in the first step. The quartz ampule was heated to 800 °C, kept at this temperature for 50 h, and then cooled to 400 °C slowly. The phase of obtained single crystals was characterized by x-ray diffraction (XRD) on a PANalytical diffractometer with Cu Kα radiation at room temperature and atmospheric pressure. The elemental compositions were checked by Oxford X-Max energy dispersive x-ray (EDX) spectroscopy analysis in a Hitachi S-4800 scanning electron microscope. Electrical resistivity was measured by the conventional dc four-probe method and the measurements were performed on a Quantum Design physical properties measurement system (PPMS-9). Samples were pressurized in a piston cylinder device made of Be–Cu alloy. The pressure transmitting medium was Daphene Oil 7373. The pressure inside the device was determined by shifting the superconducting transition temperature of Pb strip.

3. Results and discussion

In Fig. 1(a), the powder XRD pattern of $CaAs_3$ can be well indexed to the triclinic $P\bar{1}$ structure with the lattice parameters $a = 5.88(1)$ Å, $b = 5.85(1)$ Å, and $c = 5.93(1)$ Å, $\alpha = 70.05(1)°$, $\beta = 80.16(1)°$, and $\gamma = 75.83(1)°$, which are in agreement with the previous reported values.[25] Figure 1(b) shows the single crystal XRD pattern of the $CaAs_3$. All of peaks can be identified as the $(0k0)$ reflections. For comparison, we also show the crystal structure of BP in Fig. 1(c). BP is a two-dimensional (2D) layered material which is stacked together by weak van der Waals force. Each P atom is covalently bonded with three adjacent P atoms to form a puckered honeycomb structure in a single layer. One can clearly see that the crystal structure of $CaAs_3$ is similar to that of BP. Here $CaAs_3$ can be viewed as a list of 2D infinite puckered polyanionic layers As_3^{2-} stacking along the b-axis and Ca^{2+} cations are inserted into the interstitial sites, in which the puckered arsenic layers are directly derived from the orthorhombic structure of BP by removing 1/4 of the P atoms in an ordered way.[23]

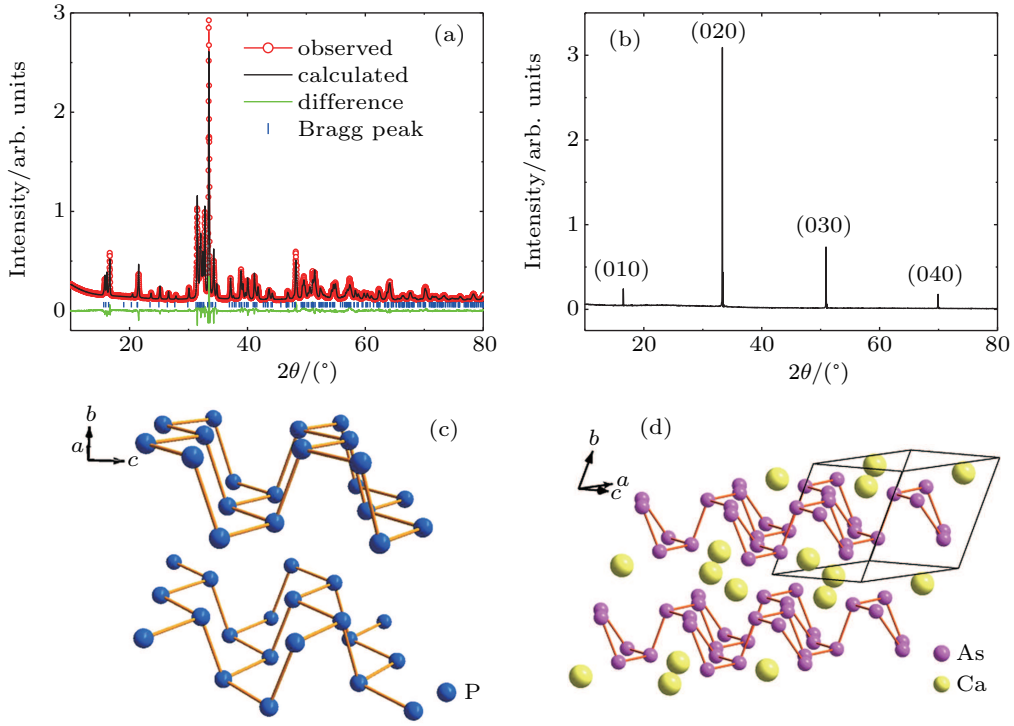


Fig. 1. (a) Powder XRD pattern of $CaAs_3$ obtained by grinding the single crystals at room temperature and the refinement results. (b) The single crystal XRD of $CaAs_3$. (c) and (d) The crystal structure of BP and $CaAs_3$, respectively.

All the samples we measured were taken from different parts of a large crystal of $CaAs_3$. We find that the transport properties show a large sample dependence. The crystals peeled from the bottom exhibit semiconducting-like behavior, while some crystals taken from the top show "bad metal" behavior with a big hump at the temperature T_1, as shown in Figs. 2(a) and 2(b), respectively. It is noted that the absolute value of resistivity is essentially same between

samples #1 and #2 at 300 K. In Fig. 2(a), the $\rho(T)$ in the range from 195 K to 265 K can be fitted by Arrhenius equation, $\rho = \rho_0 \exp(E_g/k_B T)$, where k_B is the Boltzmann constant. The estimated activation energy E_g is ~ 73 meV, which is consistent to the previous report.[22]

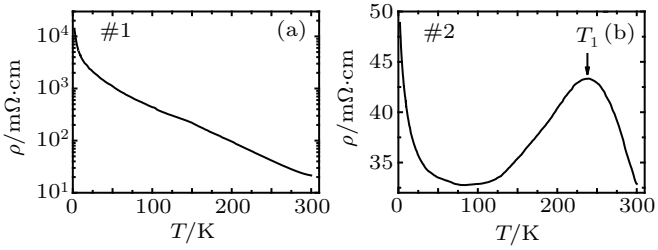


Fig. 2. Resistivity ρ plotted as a function of temperature T measured on #1 crystal (a) and #2 (b) at atmospheric pressure, respectively.

To further distinguish between the two type resistivity behaviors in the single crystals (#1 and #2) of $CaAs_3$, we performed the Hall-effect measurements at various temperatures on the same samples, as shown in Figs. 3(a) and 3(d), respectively. The magnetic field is applied perpendicular to the ac-plane. Figure 3(a) presents the magnetic field dependence of the Hall resistivity ρ_{xy} of the crystal (#1) at several temperatures from 2 K to 300 K. The slope of the ρ_{xy} curve is all negative, suggesting that the main carriers should be electron-type. One can find that the ρ_{xy} shows nonlinear behavior at 2 K, indicating the coexistence of two types of carriers at very low temperatures.[8,9] Different from sample #1, the slope of ρ_{xy} for sample #2 changes from negative to positive with decreasing temperatures, as shown in Fig. 3(d), indicating the transition from electrons dominated transport to holes dominated transport in this sample. All these show that $CaAs_3$ is a multiband system. We try to fit the Hall data obtained at 2 K for sample #1 using the semi-classical two-band model, in which Hall conductivity σ_{xy} can be expressed as the following equation:[26]

$$\sigma_{xy} = \left[\frac{n_h \mu_h^2}{1+(\mu_h B)^2} - \frac{n_e \mu_e^2}{1+(\mu_e B)^2}\right] eB, \qquad (1)$$

where n_h (or n_e) is the carrier density of the holes (or the electrons) and μ_h (or μ_e) is the mobility of the holes (or the electrons), respectively. For high temperatures, the ρ_{xy} appears to be approximately linear, and fitting with two-band model could bring uncertainty. Hence, we use the single-band model to estimate the carrier density $n_t = 1/eR_H$, and carrier mobility $\mu_t = R_H/\rho(0\ \mathrm{T})$, where t = e, h indicate electron-type and hole-type carriers, respectively, and the Hall coefficient R_H is estimated by the slope of $\rho_{xy}(B)$ at low fields ($-1\ \mathrm{T} < B < 1\ \mathrm{T}$). By fitting with the single-band and two-band model for different temperatures, the carrier densities and mobilities for sample #1 are summarized in Figs. 3(b) and 3(c), respectively. A large discrepancy is found between the results obtained from the two methods. At 2 K, the concentration and mobility for two kinds of carriers have little difference ($n_e \simeq 3.5 \times 10^{15}$ cm^{-3}, $n_h \simeq 3.2 \times 10^{15}$ cm^{-3}, $\mu_e \simeq 164$ cm^2·V^{-1}·s^{-1}, and $\mu_h \simeq 170$ cm^2·V^{-1}·s^{-1}). However, the results of fitting with single-band and two-band model are not consistent between 2 K and other temperatures. Above 20 K, μ_e increases monotonically with increasing temperature, and up to around 302 cm^2·V^{-1}·s^{-1} at 300 K, while n_e shows a little temperature dependence from 4.2×10^{17} cm^{-3} at 20 K to 9.6×10^{17} cm^{-3} at 300 K. The temperature dependence of the carrier densities and mobilities for sample #2 are shown in Figs. 3(e) and 3(f), respectively. We find that the carrier density is larger than that of sample #1 by 1 order of magnitude. The carriers change from hole-type to electron-type as the temperature goes up to around 230 K, and the transition point is in accord with T_1 in the $\rho(T)$ curve. Remarkably, the obvious hump in the $\rho(T)$ curve of the #2 crystal could be attributed to dominated carriers change. We noted that the resistivity curve of $HfTe_5$ also showed a huge hump at about 65 K, at which the dominated carrier type changed, and which was ascribed to the occurrence of the critical topological phase transition.[27] However, in this special case of layered crystal structure, the anomalous transport properties observed in some $CaAs_3$ could be reasonably attributed to the presence of impurities or crystal defects during the crystal growth.

$CaAs_3$ was predicted to hold engineered topological phase transitions by applying external tensile or compressive strains.[24] In order to test the pressure effect of $CaAs_3$, we use the piston cylinder device to apply compressive strains to two samples #3 and #4 which are selected with two typical transport behaviors. Figures 4(a) and 4(b) display the temperature dependence of the resistivity $\rho(T)$ under varying hydrostatic pressures for samples #3 and #4, respectively. The values of $\rho(T)$ both for samples #3 and #4 decrease in its entirety under pressure. At low temperatures, the $\rho(T)$ both for two samples changes more significantly, but not metallized up to 2 GPa. In Fig. 4(b), the peak temperature, T_1, also shifts to lower temperatures with increasing pressure, while we find that $\rho(T)$ of sample #4 drops with the lowering temperature above 1.5 GPa as shown in the inset. The transition moves to higher temperature with the increasing pressure. It seems natural to ascribe this drop to the onset of superconductivity in such "doped" sample, which provides the possibility for $CaAs_3$ to realize a topological nodal-line semimetal or even topological superconductivity under much higher pressure in the future work.

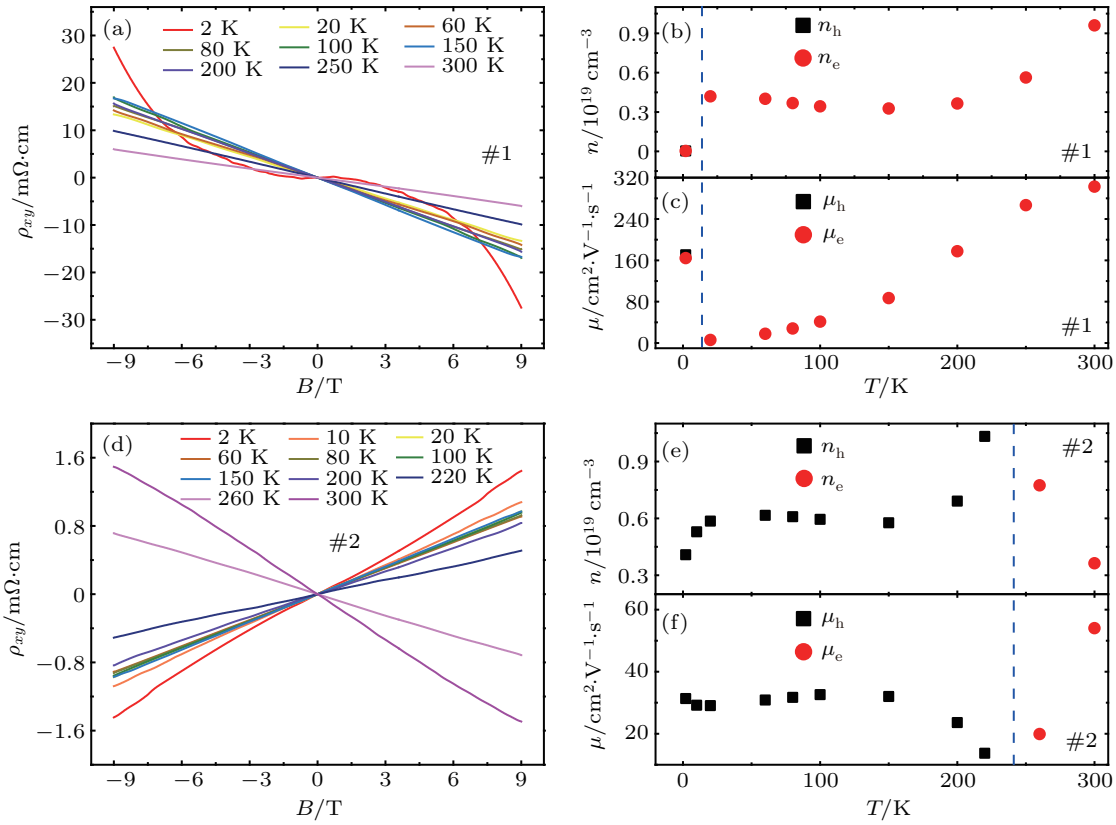


Fig. 3. (a) and (d) The magnetic field dependence of Hall resistivity ρ_{xy} on samples #1 and #2 at various temperatures, respectively. (b), (c), (e), and (f) The temperature dependence of carrier mobilities and carrier densities of electrons and holes measured on samples #1 and #2, respectively.

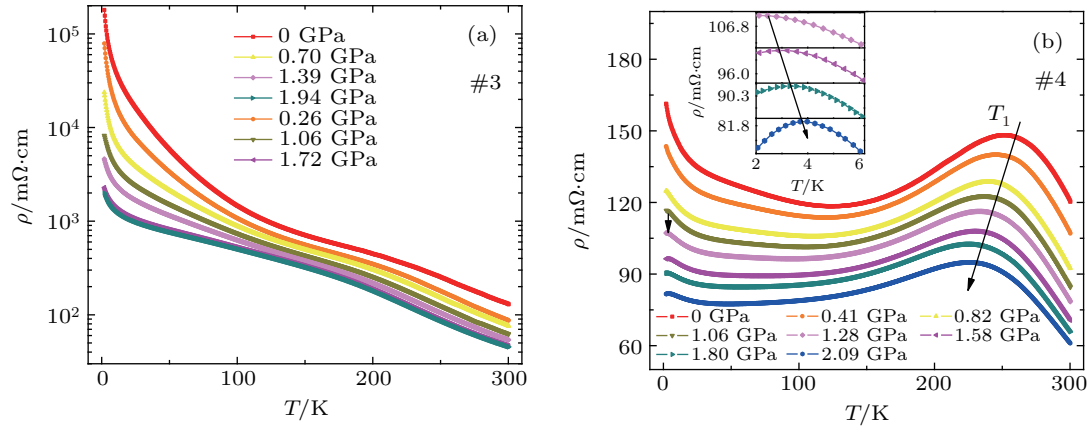


Fig. 4. (a) and (b) Resistivity ρ of $CaAs_3$ plotted as a function of temperature T on #3 and #4 crystals at various hydrostatic pressures, respectively. Inset of (b): Resistivity ρ above 1.2 GPa in the low temperature region (2 K–6 K).

4. Conclusion

In summary, we have synthesized the single crystals of $CaAs_3$, which has been predicted to be a topological nodal-line semimetal candidate. $CaAs_3$ shows an n-type semiconducting-like behavior at atmospheric pressure. While for some samples with the presence of crystal defect and/or impurities, the resistivity shows an obvious hump around 230 K, at which the dominated carriers change from hole-type to electron-type. The application of hydrostatic pressure results in decrease of the resistivity for both samples, but they are not fully metallized on the whole. A possible superconducting transition is also observed in some "doped" samples above 1.5 GPa. Our work will provide valuable clues for further exploration of the topological phase in $CaAs_3$, and in-depth studies are needed in future.

References

[1] He J B, Chen D, Zhu W L, Zhang S, Zhao L X, Ren Z A and Chen G F 2017 *Phys. Rev. B* **95** 195165
[2] Weng H M, Dai X and Fang Z 2016 *J. Phys.: Condens. Matter* **28** 303001
[3] Bansil A, Lin H and Das T 2016 *Rev. Mod. Phys.* **88** 021004
[4] Chiu C K, Teo J C Y, Schnyder A P and Ryu S 2016 *Rev. Mod. Phys.* **88** 035005

[5] Xu Q N, Yu R, Fang Z, Dai X and Weng H M 2017 *Phys. Rev. B* **95** 045136

[6] Xiong J, Kushwaha S K, Liang T, Krizan J W, Hirschberger M, Wang W, Cava R J and Ong N P 2015 *Science* **350** 413

[7] Liu Z K, Zhou B, Zhang Y, Wang Z J, Weng H M, Prabhakaran D, Mo S K, Shen Z X, Fang Z, Dai X, Hussain Z and Chen Y L 2014 *Science* **343** 864

[8] Liang T, Gibson Q, Ali M N, Liu M H, Cava R J and Ong N P 2015 *Nat. Mater.* **14** 280

[9] Huang X C, Zhao L X, Long Y J, Wang P P, Chen D, Yang Z H, Liang H, Xue M Q, Weng H M, Fang Z, Dai X and Chen G F 2015 *Phys. Rev. X* **5** 031023

[10] Zhang C L, Xu S Y, Belopolski I, Yuan Z J, Lin Z Q, Tong B B, Bian G, Alidoust N, Lee C C, Huang S M, Chang T R, Chang G Q, Hsu C H, Jeng H T, Neupane M, Sanchez D S, Zheng H, Wang J F, Lin H, Zhang C, Lu H Z, Shen S Q, Neupert T, Hasan M Z and Jia S 2016 *Nat. Commun.* **7** 10735

[11] Soluyanov A A, Gresch D, Wang Z J, Wu Q S, Troyer M, Dai X and Bernevig B A 2015 *Nature* **527** 495

[12] Cai P L, Hu J, He L P, Pan J, Hong X C, Zhang Z, Zhang J, Wei J, Mao Z Q and Li S Y 2015 *Phys. Rev. Lett.* **115** 057202

[13] Burkov A A, Hook M D and Balents L 2011 *Phys. Rev. B* **84** 235126

[14] Weng H M, Liang Y Y, Xu Q N, Yu R, Fang Z, Dai X and Kawazoe Y 2015 *Phys. Rev. B* **92** 045108

[15] Xiang Z J, Ye G J, Shang C, Lei B, Wang N Z, Yang K S, Liu D Y, Meng F B, Luo X G, Zou L J, Sun Z, Zhang Y and Chen X H 2015 *Phys. Rev. Lett.* **115** 186403

[16] Li C H, Long Y J, Zhao L X, Shan L, Ren Z A, Zhao J Z, Weng H M, Dai X, Fang Z, Ren C and Chen G F 2017 *Phys. Rev. B* **95** 125417

[17] Rodin A S, Carvalho A and Castro Neto A H 2014 *Phys. Rev. Lett.* **112** 176801

[18] Li D A, Jussila H, Karvonen L, Ye G J, Lipsanen H, Chen X H and Sun Z P 2015 *Sci. Rep.* **5** 15899

[19] Morita A 1986 *Appl. Phys. A* **39** 227

[20] Takao Y, Asahina H and Morita A 1981 *J. Phys. Soc. Jpn.* **50** 3362

[21] Asahina H, Shindo K and Morita A 1982 *J. Phys. Soc. Jpn.* **51** 1193

[22] Bauhofer W, Wittmann M, Gmelin E and van Schnering H G 1982 *Physics of Narrow Gap Semiconductors* (Berlin Heidelberg: Springer) p. 30

[23] Bauhofer W, Wittmann M and Vonschnering H G 1981 *J. Phys. Chem. Sol.* **42** 687

[24] Quan Y, Yin Z P and Pickett W E 2017 *Phys. Rev. Lett.* **118** 176402

[25] Brice J F, Courtois A, Protas J and Aubry J 1976 *J. Sol. St. Chem.* **17** 393

[26] Ashcroft N W and Mermin N D 1976 *Solid Sate Physics* (New York: Holt, Rinehart and Winston)

[27] Zhao L X, Huang X C, Long Y J, Chen D, Liang H, Yang Z H, Xue M Q, Ren Z A, Weng H M, Fang Z, Dai X and Chen G F 2017 *Chin. Phys. Lett.* **34** 037102